MODIFIED ULTRASOUND SOURCE FOR LONG FOCUSED SECOND HARMONIC BEAM

S. Saito[+] and T. Kawagishi[#]
+School of Marine Science and Technology, Tokai University, Shizuoka, JAPAN
Medical Systems Company, Toshiba Corporation, Otahara, JAPAN
ssaito@scc.u-tokai.ac.jp

Abstract

Intending to avoid the concentration of second harmonic generation on the focus, a modified focusing source designed to minimize the fundamental amplitude at the focus is examined by theory and experiment. The present source consists of coaxially arranged two confocal transducers; an inner disk transducer and an outer ring transducer whose areas are the same as each other. They have been polarized in the thickness direction opposed to each other, and are connected parallel. A relatively sharp beam of the second harmonic is demonstrated. Provided a curvature radius is relatively small, since three maximum positions are close to each other, the second harmonic beam effectively focuses long. Suppression of side lobes by weighted source excitation is also referred.

Introduction

A lateral resolution is an important factor to make a high quality ultrasonic imaging. A focusing source is often employed to get very high lateral resolution. The sound radiated from a concave source is concentrated at the focus, which is the curvature center of the source. A beam as narrow as a few wavelengths is easily obtained at the focal region. However, since the sound beam spreads outside the focal region, the high lateral resolution is obtained only near the focus. In order to eliminate such a disadvantage of focusing source, a manner called dynamic focusing is used[1]. The position of focal point is variable with weighted delay. When the acoustic images for different focal regions are joined together, the lateral resolution is effectively enhanced over a wide frame. On the other hand, a nonlinearly generated second harmonic beam is utilized for acoustic imaging[2]. The second harmonic makes a narrower beam with lower side lobes compared to the ordinary fundamental sound. However, the second harmonic beam is also wide outside the focal region. This property of the second harmonic beam may be a result of virtual source distribution. There exist three kinds of effects in an ordinary focused sound field. First, since the sound amplitude is small in the pre-focal region, the nonlinear generation is small there. This causes the small amplitude of the second harmonic sound in the pre-focal region. Secondly, the second harmonic generated in the pre-focal region also concentrates at the focus. In addition, thirdly, a large second harmonic sound is generated in the focal region. The latter two effects cause the narrow beam and large amplitude of the second harmonic sound within the focal region[3].

In the present article, a new focusing source to reduce the above inconvenience is presented. Since the degradation of lateral resolution outside a focal region is caused in part by intense virtual sources localized at the focus, a focusing source modified to decrease the fundamental amplitude at the focal point is examined by theory and experiment.

Theory and Experimental Arrangement

As shown in Fig.1, a concave source is divided into two parts. An outer ring source is opposite in phase with an inner disk source. The surface areas of two sources are designed equal to each other so that the linear sound vanishes at the focus. Assuming the boundary condition for the acoustic pressure at z=0 of $p_0\exp(-jkr^2/2D)\exp(-j\omega t)$ for $r\le a$, $-p_0\exp(-jkr^2/2D)\exp(-j\omega t)$ for $a<r\le b$ and 0 for $r>b$, the fundamental pressure $p_1\exp[j(kz-\omega t)]$ and the second harmonic pressure $p_2\exp[j2(kz-\omega t)]$ are given by the successive approximation solution for the KZK equation as follows[4,5]:

$$p_1 = -j\frac{kp_0}{z}\exp\left(j\frac{kr^2}{2z}-\alpha_1 z\right)\int_0^\infty Q_1(x)u(x)x\,dx, \quad (1)$$

$$p_2 = j\frac{\beta k^3 p_0^2}{2\pi\rho_0 c_0^2 z}\exp\left(j\frac{kr^2}{z}-\alpha_2 z\right)\times \int_0^\pi\int_0^\infty\int_0^\infty Q_2(x,y,\phi)u(x)u(y)xy\,dx\,dy\,d\phi, \quad (2)$$

where k is the fundamental wavenumber ω/c_0, ρ_0 is the density, β is the acoustic nonlinearity coefficient, α_1 is the attenuation coefficient at the fundamental frequency, and α_2 is the attenuation coefficient at the

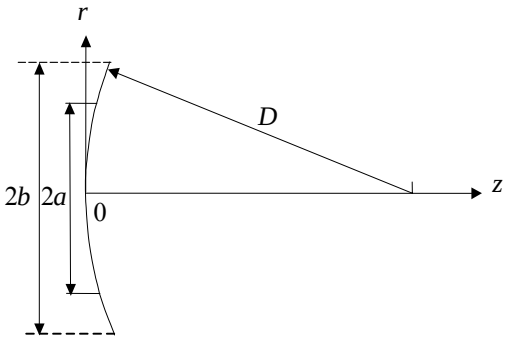

Figure 1: Geometry and notation.

second harmonic frequency. In addition,

$$Q_1(x) = \exp[\,j\frac{kx^2}{2}(\frac{1}{z}-\frac{1}{D})]J_0(\frac{kx}{z}r)$$

$$Q_2(x,y,\phi) = \exp[\,j\frac{k}{2}(x^2+y^2)(\frac{1}{z}-\frac{1}{D})]$$

$$\times[(1+j\alpha' S)\exp(-j\frac{S}{z})E_1(-j\frac{S}{z})-\alpha' z]J_0(\frac{kr}{z}\sqrt{F})$$

with $F=x^2+y^2-2xy\cos\phi$, $S=k(x^2+y^2+2xy\cos\phi)/4$ and $\alpha'=\alpha_2-2\alpha_1$. Further, $u(x)$ describes the source pressure distribution at radial distance x, and is defined as 1, -1 and 0 for $x\le a$, $a<x\le b$ and $b<x$, respectively.

The experiment is conducted in water with a 1.9-MHz piezoelectric concave source with a geometrical focal length of D=85 mm. The source consists of an inner disk transducer with 32-mm aperture diameter and an outer ring transducer with 34-mm inner diameter and 47-mm outer diameter. They have been polarized in the direction opposite to each other. They are connected in parallel and simultaneously driven by tone bursts with 20-μs duration and 1-kHz repetition rate. The pressure distribution is measured with a needle type PVDF hydrophone, where the source pressure p_0 is set at 7.5×10^4 Pa.

Experimental Result

Figure 2 shows the acoustic pressure distribution on the axis. The experimental plots are compared with the solid curve of computation assuming a=16.5 mm and b=23.5 mm. The experimental result reasonably agrees

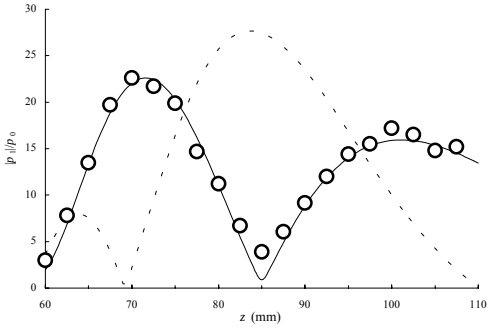

(a) Fundamental amplitude

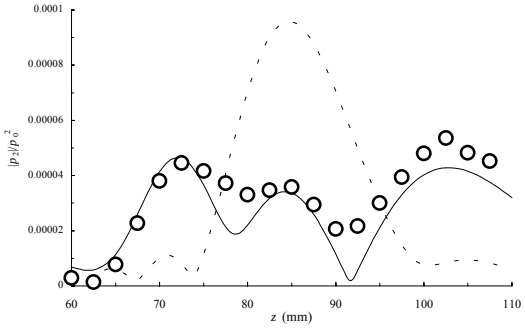

(b) Second harmonic

Figure 2: Acoustic pressure on the axis.

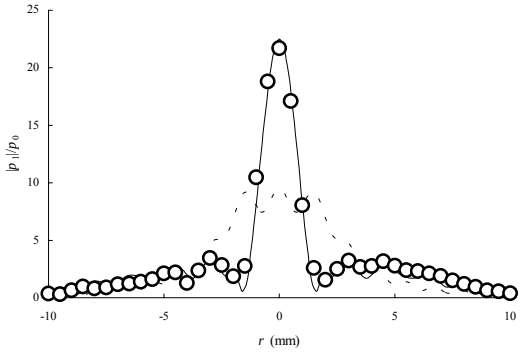

(a) z=72.5 mm

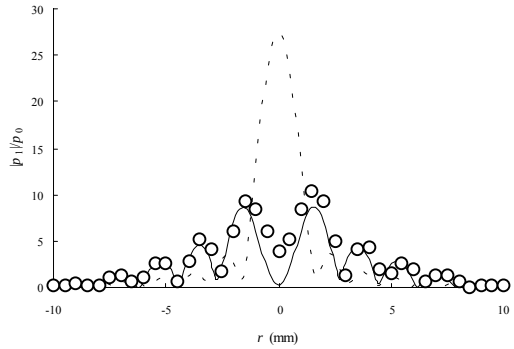

(b) z=85 mm

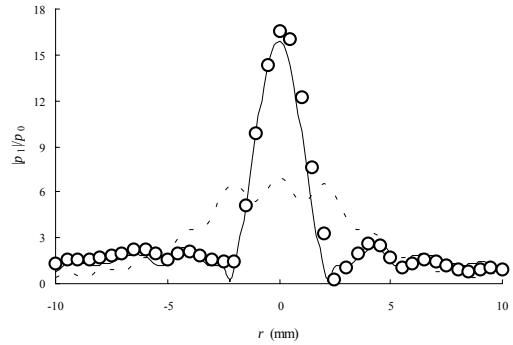

(c) z=102.5 mm

Figure 3: Fundamental amplitude on the plane perpendicular to the axis.

with the theoretical. The fundamental component almost vanishes at the focus, and attains maximum at two other positions z=72.5 mm and z=102.5 mm. The dotted curve calculated for an ordinary focusing source with the same outer radius is also shown for comparison. Since the second harmonic radiation of the virtual sources in the prefocal region concentrates at the focus, the third maximum appears in addition to two fundamental maximum positions. Then the second harmonic amplitude becomes almost uniform along wider axial ranges.

The lateral distribution of the fundamental pressure at two maximum positions and at the geometrical focus is shown in Fig.3. Many side lobes appear at z=85 mm. Including the representation of this phenomenon, the experimental result agree well with the calculation. Comparing with an ordinary focusing source, a sharp beam with greater amplitude is attained at z=72.5 mm and z=102.5 mm.

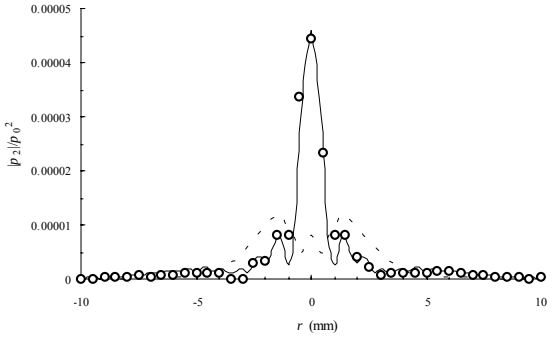

(a) z=72.5 mm

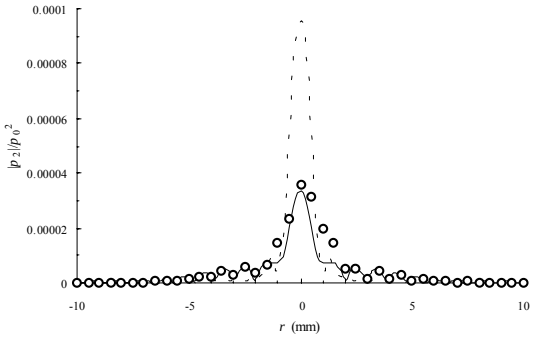

(b) z=85 mm

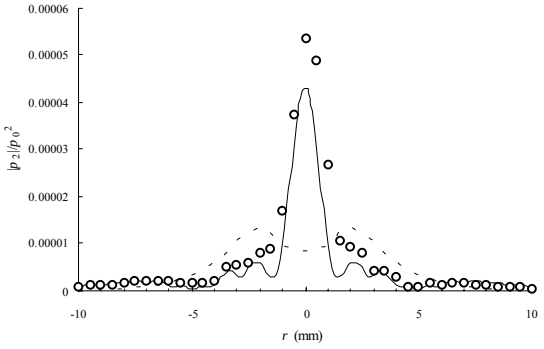

(c) z=102.5 mm

Figure 4: Second harmonic amplitude on the plane perpendicular to the axis.

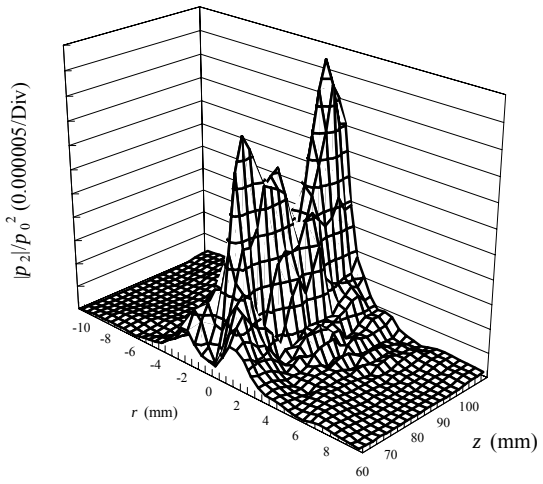

(a) Experiment

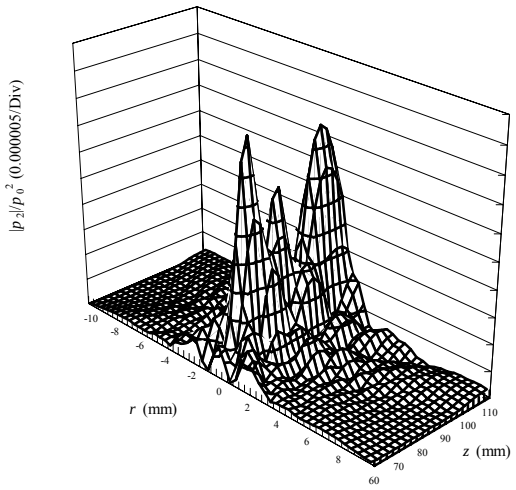

(b) Theory

Figure 5: Two dimensional display of second harmonic amplitude.

The lateral distribution of the second harmonic pressure at three maximum positions is also shown in Fig.4 where a reasonable agreement between the experiment and calculation is demonstrated. The beam is much narrower than that of the conventional focusing source indicated by the dotted curves particularly out the focal region. The beam is narrow over the measured regions though the side lobes are slightly large.

Figure 5 illustrates the measured distribution of the second harmonic amplitude within the range of 60 mm≤z≤110 mm and r≤10 mm. It is found that, around the focal plane, a narrow beam can be formed over a relatively wide range together with the third maximum, as mentioned above, formed by a focused second harmonic sound generated in the prefocal region. The experimental result agrees well with the theoretical prediction.

Additional Analysis

Through the comparison between theory and experiment, it was confirmed that Eqs.(1) and (2) are useful to predict the sound field. Then, assuming the similar inner transducer radius a, outer transducer radius b and fundamental frequency, the acoustic field of the present modified source is computed for different curvature radii D such as 140 mm and 220 mm. Figures 6(a) and 6(b) show the two dimensional distribution of the second harmonic pressure. In the case of the curvature center is relatively close to the source as in the present experiment, the distance between two maximums of the fundamental component becomes relatively small. Two maximums of second harmonic sound created at two maximum positions for the fundamental are then connected to each other by being bridged with another maximum of the second harmonic sound

appearing at the curvature center of the source. However, when the curvature center is distant from the source as in the case of Fig.6(b), two maximum points of second harmonic sound are too far from each other to be bridged. In addition, the weak focusing due to the large curvature radius cannot generate the second harmonic sound enough to cover the space between two maximum points. Accordingly an ordinary focusing source makes rather narrow beam of second harmonic sound over wide range in a case of large D/b value.

Replacing the distribution function in Eqs.(1) and (2) for $0 \le x \le b$ with $u(x)=1/[1+\exp\xi(x-a)]-1/[1+\exp\xi(a-x)]$, the acoustic field of the second harmonic is calculated for the modified source whose source amplitude is shaded around the radial distance $r=a$. The result for weighting coefficient ξ of 200 m^{-1} is shown in Fig.7. Since the condition to vanish the linear pressure amplitude at the curvature center is almost retained after the shading, the second harmonic field is similar to Fig.5 for the non-shaded source. However the relative levels of both the pressure amplitude far from the axis and the side lobes are lower. The average amplitude is decreased according to the lower source level caused by shading.

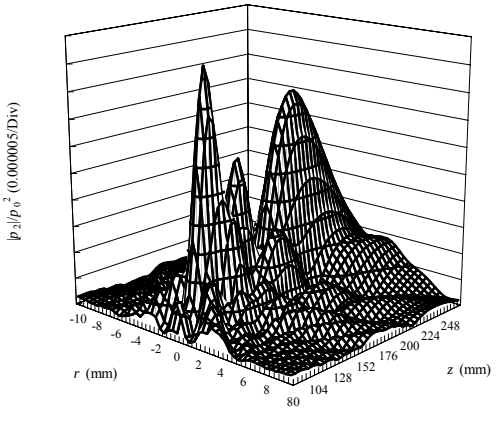

(a) D=140 mm

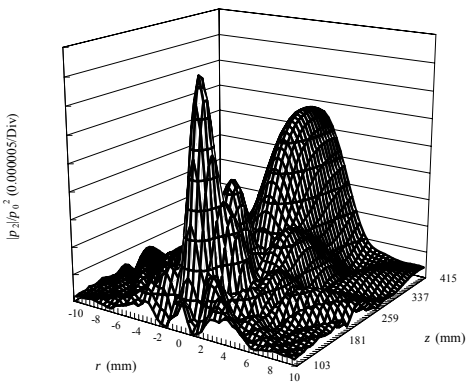

(b) D=220 mm

Figure 6: Second harmonic distribution for modified focusing source with different curvature radius.

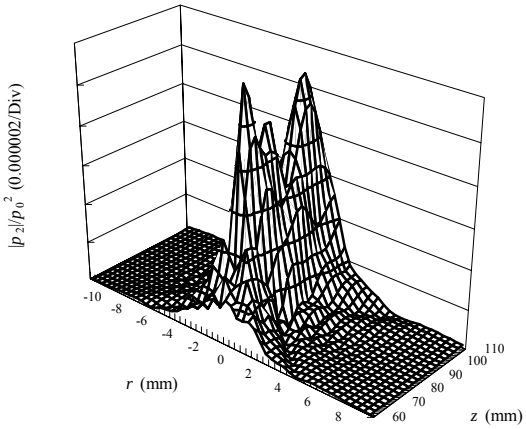

Figure 7: Computed distribution of the second harmonic generated by a shaded source.

Conclusion

The second harmonic sound in the newly proposed focusing source was experimentally and theoretically examined. Two maximums appear for the fundamental at the axial positions excluding the geometrical focal point. Since the second harmonic component attains maximum at three positions including the focal point, the distribution of the second harmonic sound becomes almost uniform. Then the beam is relatively narrow over wider ranges around the focal region. The present source may be useful to obtain a long narrow beam near the source.

References

[1] K. Saito, "Sound field of electronic scanning type diagnostic system," Handbook of Ultrasonic Diagnostic Equipments, pp. 42-44, Corona Publishing, Tokyo, 1997 [in Japanese].

[2]M. A. Averkiou, D. N. Roundhill and J. E. Powers, "A new imaging technique based on the nonlinear properties of tissues," Proc. IEEE Ultrason. Symp. Toronto, October 1997, pp. 1561-1566.

[3] S. Saito and B. C. Kim, "Selective detection of second harmonic sound generated at the focal region in a finite amplitude focusing field," J. Acoust. Soc. Jpn. vol. 8, pp. 167-175, 1987.

[4] S. Saito, B. C. Kim and T. G. Muir, "Second harmonic component of a nonlinearly distorted wave in a focused sound field," J. Acoust. Soc. Am. vol. 82, pp.621-628, 1987.

[5] S. Saito, N. Akashi and J. Kushibiki, "Second harmonic component of nonlinearly distorted wave in a 20-MHz focused sound field," J. Acoust. Soc. Jpn. vol. 19, pp.133-139, 1998.